Features of lateral energy transport in CO_2-laser-irradiated microdisk targets

D. M. Villeneuve, G. D. Enright, and M. C. Richardson*

Division of Physics, National Research Council of Canada, Ottawa, Canada K1A 0R6

Calorimetric investigations of the lateral flow of energy away from CO_2-laser-irradiated regions of disk targets are reported. The fraction of energy reaching the rear surface is shown to decrease with increasing target diameter, but does not depend on target thickness. Most of the plasma blow-off energy in front of the target is due to fast ions, but these account for less than 20% of the rear blow-off energy. The rear surface is heated preferentially at the edges, in the plane of laser polarization. These observations are consistent with energy being transported laterally by hot electrons inside the corona which expands at a speed of $\sim 10^8$ cm/s.

INTRODUCTION

Studies of nanosecond CO_2-laser interaction with solid targets at high intensities have established that absorption of the laser radiation occurs primarily through resonance absorption[1] which accelerates superthermal electrons through the critical density surface. The production of these energetic electrons is problematical for laser fusion schemes in that a sizable fraction of the absorbed energy is transferred to a population of fast ions which do not aid in pellet compression. In addition, owing to their long mean-free paths, the hot electrons may preheat the shell and fuel, thus reducing the peak fuel density. Since hot electrons dominate the energy balance, it is important to understand their behavior during CO_2-laser-plasma interaction.

The resonance absorption process accelerates electrons down the density gradient, producing an approximately Maxwellian distribution of energetic electrons.[2] These energetic electrons quickly pass beyond the outermost ions and are decelerated by the space-charge separation field. A self-consistent potential is thus set up near the ion front which reflects most of the electrons back into the dense plasma. Potentials exceeding several hundred kilovolts are possible.[3] The electrons which do escape are slowed down by the potential and are thus not representative of the coronal hot-electron distribution.

Electron motion in the corona is virtually collisionless and is determined primarily by the self-consistent fields. Each time an electron "bounces off" the potential, it transfers its momentum to the field, which in turn accelerates ions near the front, resulting in the production of fast ions. The ion front thus expands at the sound speed

$c_h = (ZT_h/M_i)^{1/2}$, where T_h is the hot-electron temperature, Z is the ionization state of the ions, and M_i is the ion mass.

Because of the mass difference between electrons and ions, the electrons will lose only a few percent of their energy on each reflection from the corona. Since up to 50% of the absorbed energy is known to be converted to fast ions,[4] many bounces are required which implies that the target surface must be somehow insulated from the flux of returning hot electrons. Azimuthal magnetic fields[5] may do this by making the hot electrons spiral in the corona. Evidence for such fields has been obtained[6] under similar conditions.

Resonantly accelerated electrons therefore can (a) escape the target potential, (b) accelerate fast ions, or (c) penetrate the dense material. In the latter case, they may either be thermalized or reflected outwards again. For spherical targets, the corona expands radially outwards,[7] and as it gets larger, the electrons become more decoupled from the target. For flat targets, the corona also expands laterally away from the focal spot. For $T_h = 20$ keV, $c_h = 10^8$ cm/s, and so during a 1-ns pulse, the corona can expand several millimeters. Since the electrons move rapidly and collisionlessly in the corona, a sizable fraction of the absorbed energy may be transported millimeters from the laser focus.

The effects of these hot electrons have become apparent in various experiments. Energy loss to fast ions has been observed with disk targets,[8] and the total fast-ion loss has been shown to be $\sim 50\%$ of the absorbed energy for spherical targets.[4] Escaping energetic electrons of up to 600-keV energy have been detected on both sides of disk targets.[9] The hard x rays produced when the electrons impinge on the dense target material extend to over 900 keV,[10]

and the electron range into aluminum has been shown to be <4 μm.[11]

It is the purpose of the paper to report investigations of the expansion of the superthermal corona from disk targets irradiated by nanosecond CO_2-laser pulses.

EXPERIMENTAL CONDITIONS

In the present experiments, one beam of the COCO-II CO_2-laser system was employed.[12] The 10.6-μm pulse had a rise time of 300 ps and a fall time of ~ 1 ns. Prepulse energy was less than 50 μJ. Most of the targets were irradiated with a beam of intensity $\leq 10^{14}$ W/cm^2, whose half-energy focal-spot diameter was 110 μm. The $f/2.5$ beam was incident at 22° from target normal. The targets were disks of various metals, from 0.5- to 20-mm diam, with thicknesses ranging from 0.7 to 125 μm. Except where noted, the disks were glued on the ends of 20-μm glass stalks.

The asymptotic plasma blowoff was measured by means of an array of 20 plasma calorimeters.[13] These devices measure the total energy intercepted by the detector in the form of ions, electrons, neutral particles, and x rays. For the present studies, however, the x-ray flux (> 1 keV) contributes much less than 1% of the absorbed energy,[14] and can, therefore, be neglected. The plasma blow-off distribution in three dimensions may be integrated to obtain the total plasma energy, which can be equated to the fraction of laser energy absorbed. Since the distribution of the scattered laser radiation was also measured by the calorimeters, it was possible to confirm the absolute calibration of all the detectors, through energy balance.

Three Thomson parabola ion spectrographs were used to characterize the asymptotic fast-ion expansion. The use of CR-39 nuclear-track detector material enabled them to be absolutely calibrated also. These measurements determine the angular dependence of the fast-ion spectra and provide an estimate for the total energy in the fast-ion expansion.

Finally, x-ray and ion pinhole imaging of the rear target surface has clearly established the extent of the heated region on the rear surface of disk targets.

RESULTS

Figure 1 shows the spatial distribution of the plasma blowoff as measured by plasma calorimetry. The polar angle is measured from the target normal axis, so that some detectors lie in the plane of polarization whereas others lie above it. The emission from the front of the target is strongly peaked, and the rear emission is even more so, suggesting that it
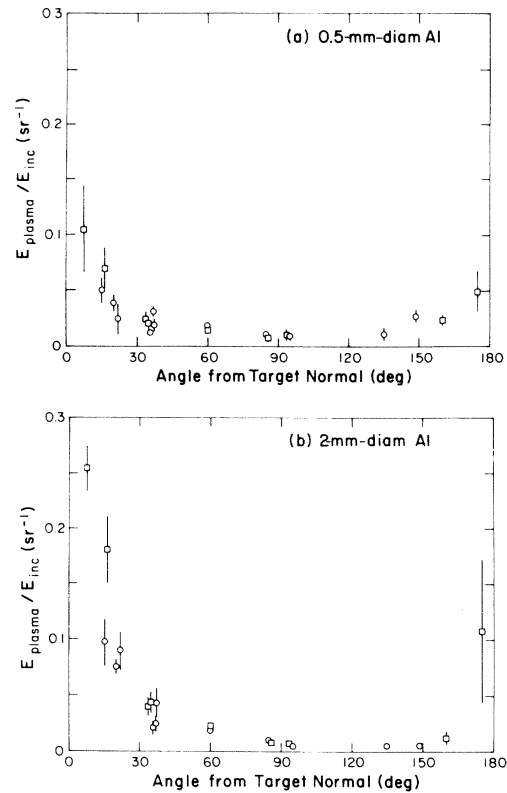

FIG. 1. Polar distribution of plasma blowoff from disk targets assuming cylindrical symmetry, normalized to the incident laser energy (E_{inc}). Error bars show range of data for three shots. Squares represent detectors whose projection of the position vector onto the target surface lay greater than 45° above the plane of polarization. (a) 0.5-mm-diam aluminum disk and (b) 2-mm-diam aluminum disk.

originates from the rear surface. Those points marked with squares represent detectors whose position vectors' projection onto the target surface was more than 45° above the plane of polarization. No asymmetry related to polarization is apparent, al-
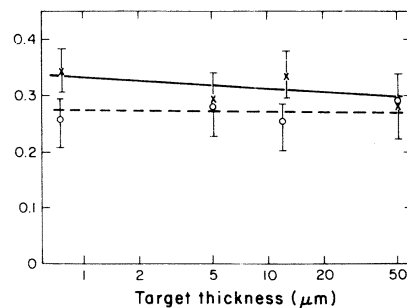

FIG. 2. Dependence of total absorption (dashed line) and fraction of absorbed energy emitted into rear hemisphere (solid line) on thickness of target, for 0.5-mm-diam aluminum targets.
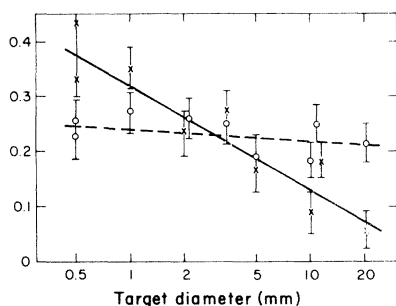
FIG. 3. Dependence of total absorption (dashed line) and fraction of absorbed energy emitted into rear hemisphere (solid line) on target diameter, for 12.5-μm-thick aluminum targets. Fraction appearing at the rear decreases with increasing target diameter.

though there are not sufficient data in the plumes to say if they are symmetric.

Figure 2 shows the dependence on target thickness of absorption (dashed line) and the fraction emitted by the rear of the target (solid line). In this case the targets were 0.5-mm-diam aluminum disks. Clearly, both total absorption and rearward emission are independent of target thickness over the range measured. This suggests that energy appearing at the rear surface cannot be transmitted through the bulk of the target. The penetration depth for a 20-keV electron in aluminum is only 3 μm (Ref. 15), and the thermal wave will progress less than a micron during the nanosecond laser pulse[11,16] (and in any case will have insufficient energy to heat the rear surface to such a degree). In addition, a shock would not have sufficient energy.[17] Thus only surface effects or coronal mechanisms could be responsible.

Figure 3 shows that the amount of energy appearing at the rear surface of aluminum targets (solid line) decreases with increasing target size, in support of the hypothesis of around-target energy transport. The fact that the total absorption (dashed line) is relatively constant implies that refraction of laser energy onto remote parts of the target is not important.
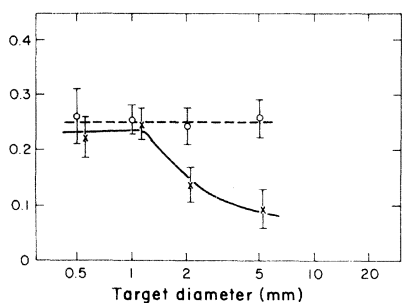

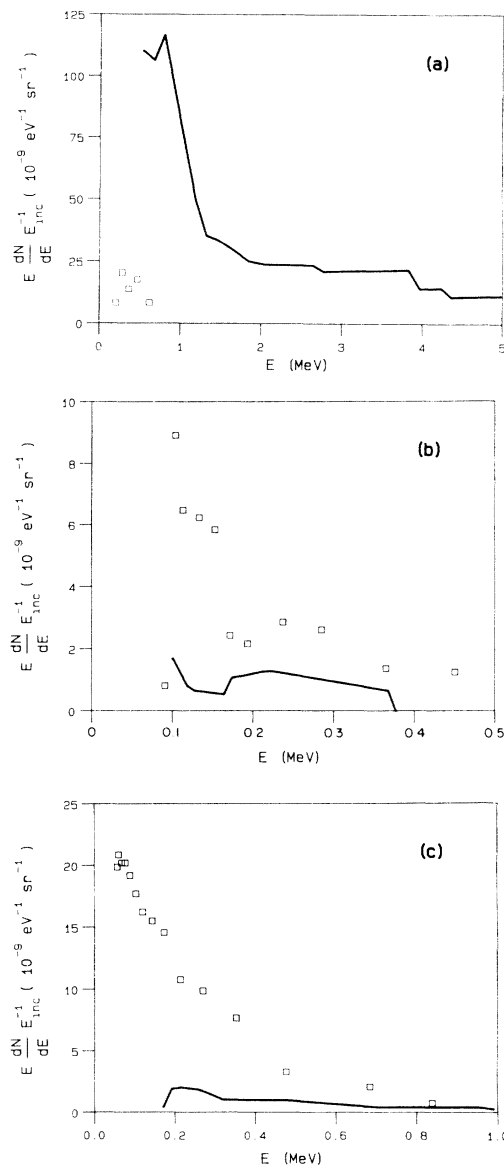FIG. 4. As in Fig. 3, except targets are 25-μm-thick gold disks of various diameters.

FIG. 5. Spectra of fast ions emitted from disk targets at (a) 0°, (b) 90°, and (c) 180° from target normal. Measurements were made with Thomson parabola ion spectrographs and CR-39 detectors. $\square$, protons; solid line, sum of all other species.

The dependence of the amount of energy appearing at the rear surface of gold targets on target diameter is shown in Fig. 4. Front-to-back ratios for gold correspond to similar ratios for aluminum at 2.5 times the target diameter. This factor is very close to the ratio of sound speeds between gold and aluminum, assuming average ionization states of 16 and 12, respectively, using[18] $Z = 3T^{0.3}$ and $T = 250$ eV. This may suggest that the rate of energy deposition on the rear surface is controlled by the velocity of the expanding plasma sheath, which has been the

subject of a recent investigation.[19] However, in both cases the predominant fast-ion species observed behind and to the side of the target were carbon and hydrogen, independent of the target composition, so that the observed differences are somewhat unexpected.

In an attempt to investigate the role of the sheath expansion velocity, some efforts were made to remove contaminants from the target surface, thereby changing the ion acoustic speed c_s. Various methods were employed, such as resistance heating of ribbon targets, and cw laser irradiation and electron-beam heating of disk targets. The hydrogen could be removed by such techniques; however, the carbon remained. There was no observable difference in the calorimetric observations with or without hydrogen, in contrast to the results quoted[20] for heated wires. This is hardly surprising since c_s would change by only a small fraction.

Metal stalks were substituted for the glass supports on which the targets were mounted, in order to determine if stalk impedance had any effect on the plasma blowoff. The total absorption, the back-to-front ratio, and the detailed blow-off distribution remained the same for both supports. This implies that stalk return currents do not have any apparent effect on the lateral energy transport, although they have been shown to greatly affect the energetic electron flux escaping the target potential.[9]

The three Thomson parabola ion spectrographs were employed to characterize the fast-ion blow-off distribution from aluminum targets of various diameters. Two of the spectrographs were situated along the target normal, in front of and behind the target. The third spectrograph probed the direction parallel to the target surface, 30° out of the plane of polarization (incident p polarized).

In the forward direction the fast-ion blowoff comprises Al^{4+} to Al^{12+} (mainly Al^{10+} and Al^{11+}) with a small contribution from C^{6+} and protons. In the rearward and sideways directions protons are dominant with additional contribution from

C^{3+}, C^{4+}, and C^{5+}. During these experiments the vacuum was $\lesssim 3\times10^{-6}$ Torr, so the probability of charge exchange occurring between the plasma and the spectrographs was small. The predominant ion species observed are consistent with a peak surface temperature of 200—300 eV on the front surface and 50—75 eV on the rear surface. It is clear from x-ray pinhole photographs that only the focal region reaches these temperatures on the front surface and, as we shall show below, it is also only a small region on the rear surface that is heated significantly.

The fast-ion spectra from 0.5-mm-diam targets are shown in Fig. 5. Here the energy emitted per steradian, normalized to the laser energy, is plotted as a function of ion energy. The protons are plotted separately from the sum of the other ion species. The spectra below ~ 200 keV for C and Al ions and below ~ 50 keV for protons are not shown due to falloff in instrument and detector sensitivity. It is clear that the spectra depend on the angle of observation. For larger-diameter targets the spectral shape is similar, although the ion flux drops to the side and behind the target and increases in front of the target. The proton spectrum obtained in front of the target appears to be broadly peaked around 300—400 keV, and clearly drops off below 200 keV, whereas the proton spectra behind and to the sides of the targets are strongly peaked around 100 keV. The protons appear to have a cut-off velocity of about 10^9 cm/s$(\sim 500$ keV$)$. The isothermal expansion model may be used to obtain a fast-ion acoustic velocity from the asymptotic velocity distributions. Assuming a planar expansion, the proton spectra obtained in the present experiment yield a sound speed of $(1.2-1.5)\times10^8$ cm/s, implying a hot-electron temperature in the range 15—25 keV. This is consistent with the inferred hot x-ray temperature obtained with detectors sensitive to x rays up to 50 keV and agrees with the time-resolved double-disk experiments of Marjoribanks et al.[19]

Integration of the individual ion spectra provides the total energy in each species, and by summing

TABLE I. Energy partition in fast ions for 0.5-mm-diam aluminum targets.

Species	$\theta=0°$ $E_{ion}/E_{inc}(\text{ sr}^{-1})$	Species	$\theta=90°$ $E_{ion}/E_{inc}(\text{ sr}^{-1})$	Species	$\theta=180°$ $E_{ion}/E_{inc}(\text{ sr}^{-1})$
H^+	6.17×10^{-3}	H^+	1.1×10^{-3}	H^+	5.69×10^{-3}
Al^{8+}	2.16×10^{-2}	C^{3+}	2.15×10^{-4}	C^{2+}	1.64×10^{-4}
Al^{9+}	4.66×10^{-2}	C^{4+}	2.34×10^{-4}	C^{3+}	1.0×10^{-4}
Al^{10+}	4.51×10^{-2}			C^{4+}	6.4×10^{-4}
Al^{11+}	2.88×10^{-2}				
Al^{12+}	1.38×10^{-2}				
Total	1.62×10^{-1}		1.55×10^{-3}		6.59×10^{-3}
Total plasma	1.30×10^{-1}		9.5×10^{-3}		5.0×10^{-2}

over each species the total energy in the fast-ion expansion can be obtained for the three directions probed. Table I gives the energy emitted per steradian, normalized to the laser energy, for the predominant ion species observed from the 0.5-mm-diam targets. The uncertainties in the values listed are approximately ±15% and are due to the accuracy in determining the origin and the deflection axes as well as the extrapolation procedures used in the integration of the individual ion spectra. The shot-to-shot variation fell well within this uncertainty except at $\theta = 0°$ where larger fluctuations (up to ±30%) from shot to shot were observed both in the ion spectrograph data and the plasma calorimetry. This is most probably due to inaccuracy in aligning the target normal along the axis of the chamber. The total plasma energy, obtained from calorimetry, is also shown in Table I and represents the average of three shots. For experimental reasons, the calorimeter and ion spectrograph data were collected on different shots.

In the forward direction all of the energy in the plasma blowoff, as registered by the calorimeters, can be accounted for in the fast ions. For the other directions the ratio of fast-ion energy to total plasma energy is somewhat dependent on target diameter as is shown in Fig. 6. Here the dashed line represents the fast-ion fraction observed at the sides of the target, and the solid line represents the fraction observed behind the target. In all cases only about 15% of the rear plasma blowoff can be accounted for by the fast ions.

The angular dependence of the rearward fast-ion blowoff is similar to that observed for the total plasma blowoff (Fig. 1) for the 0.5-mm-diam targets. As the target diameter is increased there is little change in the fast-ion angular distribution whereas
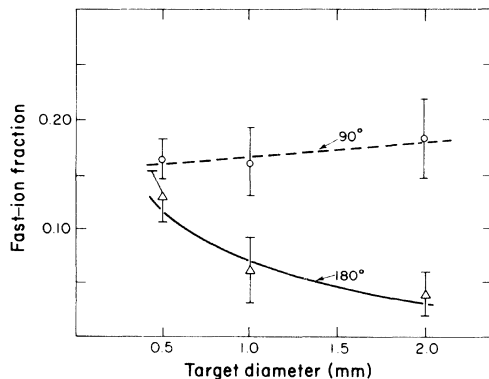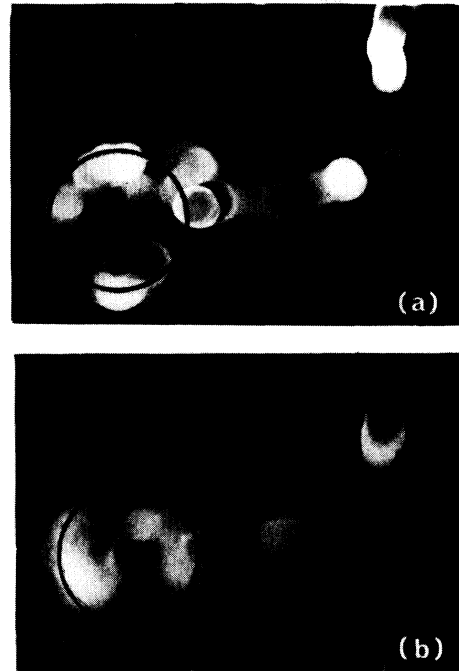

FIG. 7. Ion pinhole pictures of the rear surface of 2-mm-diam aluminum disks. Disks are mounted on L-shaped supports which extend to the right of the target and then up. Tracks due to fast ions are visible microscopically only on those bright areas on the target itself, not on the support structure. (a) Vertically polarized laser and (b) horizontally polarized laser.

FIG. 6. Fraction of total plasma flux emitted as fast ions at 90° (0) and 180° (△) from target normal. At target normal, all of the plasma flux could be accounted for in fast ions.

the total plasma blowoff becomes more strongly peaked along the target normal.

In order to estimate the total energy contained in the fast ions, the angular dependence of the fast-ion blowoff in the forward direction must be known since the fast ions are strongly peaked in this direction. Previous charge-collector studies[21] were used to estimate the angular distribution of fast ions. If the angular dependence thus inferred is normalized to the Thomson parabola data, an estimate of the total fast-ion blow-off energy can be obtained. For the 0.5-mm-diam targets we estimate that between 35% and 55% of the absorbed energy is found in the fast-ion expansion and for the 2.0-mm-diam targets this fraction rises to between 50% and 70%. The uncertainties in these estimates are due to uncertainties both in the measurement of the fast-ion fraction (~20%) and the determination of the angular extent of the fast-ion forward blow off.

Ion pinhole images of the rear surface were recorded on CR-39 nuclear-track material, in order to determine the regions of fast-ion emission. The pinhole was 350 μm in diameter and situated normal to the target surface. Figure 7 shows ion images for vertically and horizontally polarized beams.

Most of the exposure shown is due to slower ions, but individual tracks of fast ions are visible microscopically and appear only on the bright areas of the target periphery, not on the support structure. X-ray pinhole photographs have also revealed that the x-ray emitting region of the rear surface plasma is confined primarily to the disk perimeter and is enhanced in the plane of polarization. These results confirm evidence obtained from x-ray streak photography[22] and interferometry[23] that the heated region of the rear surface is confined to an annular region near the perimeter.

DISCUSSION

The observation of fast ions of energy up to 5 MeV, $K\alpha$ emission from the rear surface,[24] time-resolved interferometry,[23] and near-infrared streak photography[19] have established that the rear surface plasma is formed during the laser pulse. The streak photographs determine the velocity of energy transport to the rear surface to be about 10^8 cm/s, which corresponds to the ion acoustic speed assuming a hot-electron temperature of 20 keV inferred from continuum x-ray spectra.

It is not possible for the observed energy to be transmitted through the target on this time scale, or indeed on any time scale. Convection of plasma around the target edge was investigated using a two-dimensional momentum- and energy-conserving single-fluid Eulerian model, employing the Lax-Wendroff method. The results indicated that convection could not transport much plasma to the rear surface.

The hot electrons created in the focal region describe large orbits in the potential field surrounding the target, some traveling a large distance ahead of the ion front. Using the expression due to Crow et al.[25] for the electron density, it can be shown that the electrons which may orbit the target will deposit only a few microjoules on the rear surface. This energy is just sufficient to cause the weak emission from the rear immediately at the beginning of the laser pulse that has been observed in streak photographs.[19]

On the other hand, the corona will propagate rapidly at the fast-ion velocity away from the focal region, bringing with it the bulk of the hot electrons. These hot electrons are capable of transporting large amounts of energy and can produce more plasma by collisions with the cold target surface. Once the corona reaches the target edge, the long—mean-free-path hot electrons have a channel through which to carry energy to the rear surface. Since this occurs during the laser pulse, hot elec-

trons are continually being accelerated from the focal region, so the corona may be treated as an isothermal plasma. When the laser field turns off, the hot electrons quickly cool, and the plasma expands adiabatically. Thus energy is only transmitted as far as the sheath progresses during the laser pulse.

The observation of enhanced heating of the rear edges lying in the plane of polarization is indicative of the corona being driven preferentially in the plane of polarization. Since the hot electrons are accelerated down the density gradient and are more abundantly produced where the angle and polarization requirements for resonance absorption are met, it is expected that electrons should be produced preferentially in the plane of polarization.

Magnetic fields also play a role in the lateral expansion of the corona. Simulations[5] have shown that megagauss azimuthal magnetic fields are produced around the focal spot and tend to isolate the target surface from returning electrons. The electrons experience $E \times B$ drift along the target surface and cause enhanced lateral transport. The simulations also predict preferential heating of the rear edges, as has been observed here.

CONCLUSION

It has been shown that energy from the laser focus is transmitted laterally for distances up to 5 mm during CO_2-laser irradiation of disk targets. Plasma blowoff from the rear surface is independent of target thickness but falls off with increasing target diameter, commensurate with the greater distance that the corona must travel during the laser pulse. Fast ions make up the majority of the forward-directed plasma blowoff but contribute only a small fraction to the rearward blowoff. Preferential heating of the rear edges lying in the plane of polarization indicates the asymmetry of the hot-electron source.

These studies underline the fact that care must be exercised when using a CO_2 laser with finite spot size, since the heated region may extend millimeters beyond the focal region. For experiments which study rear surface effects of foils, adequate shielding must be used to prevent lateral energy transport around the edge of the foil.

*Present address: Laboratory for Laser Energetics, University of Rochester, Rochester, N.Y. 14623.

[1]J. P. Freidberg, R. W. Mitchell, R. L. Morse, and L. I. Rudsinski, Phys. Rev. Lett. 28, 795 (1972).

[2]K. Estabrook and W. L. Kruer, Phys. Rev. Lett. 40, 42 (1978).

[3]J. S. Pearlman and G. H. Dahlbacka, Appl. Phys. Lett. 31, 414 (1977).

[4]D. M. Villeneuve, G. D. Enright, M. D. J. Burgess, R. Fedosejevs, and M. C. Richardson, Phys. Rev. Lett. 47, 515 (1981).

[5]D. W. Forslund and J. U. Brackbill, Phys. Rev. Lett. 48, 1614 (1982).

[6]N. A. Ebrahim, M. C. Richardson, R. Fedosejevs, and U. Feldman, Appl. Phys. Lett. 35, 106 (1979).

[7]J. R. Albritton, I. B. Bernstein, E. J. Valeo, and E. A. Williams, Phys. Rev. Lett. 39, 1536 (1977).

[8]C. Joshi, M. C. Richardson, and G. D. Enright, Appl. Phys. Lett. 34, 625 (1979).

[9]N. A. Ebrahim and C. Joshi, Phys. Fluids 24, 138 (1981).

[10]W. Priedhorsky, D. Lier, R. Day, and D. Gerke, Phys. Rev. Lett. 47, 1661 (1981).

[11]J. C. Kieffer, H. Pepin, F. Martin, P. Church, T. W. Johnston, and R. Decoste, Phys. Rev. Lett. 44, 1128 (1980).

[12]M. C. Richardson, M. D. J. Burgess, N. H. Burnett, N. A. Ebrahim, G. D. Enright, R. Fedosejevs, P. A. Jaanimagi, C. Joshi, R. S. Marjoribanks, and D. M. Villeneuve, *Laser Interaction and Related Plasma Phenomena*, edited by H. J. Schwarz, H. Hora, M. Lubin, and B. Yaakobi (Plenum, New York, 1981), Vol. 5, p. 145.

[13]D. M. Villeneuve and M. C. Richardson, Rev. Sci. Instrum. 51, 306 (1980).

[14]G. D. Enright, N. H. Burnett, and M. C. Richardson, Appl. Phys. Lett. 31, 494 (1977).

[15]R. D. Evans, *The Atomic Nucleus* (McGraw-Hill, New York, 1955), p. 624.

[16]K. B. Mitchell and R. P. Godwin, J. Appl. Phys. 49, 3851 (1978).

[17]R. J. Trainor, J. W. Shaner, J. M. Auerbach, and N. C. Holmes, Phys. Rev. Lett. 42, 1154 (1979); N. H. Burnett, G. Josin, B. Ahlborn, and R. Evans, Appl. Phys. Lett. 38, 226 (1981).

[18]M. J. Bernstein and G. G. Comisar, J. Appl. Phys. 41, 729 (1970).

[19]R. S. Marjoribanks, M. D. J. Burgess, G. D. Enright, and M. C. Richardson, Phys. Rev. Lett. 45, 1798 (1980).

[20]A. W. Ehler, F. Begay, T. H. Tan, and P. H. Castine, J. Phys. D 13, L65 (1980).

[21]D. M. Villeneuve, G. D. Enright, M. C. Richardson, and N. R. Isenor, J. Appl. Phys. 50, 3921 (1979).

[22]P. A. Jaanimagi, N. A. Ebrahim, N. H. Burnett, and C. Joshi, Appl. Phys. Lett. 38, 734 (1981).

[23]M. D. J. Burgess, G. D. Enright, R. Fedosejevs, and M. C. Richardson, *Picosecond Phenomena II*, edited by R. Hochstrasser, W. Kaiser, and C. V. Shank (Springer, New York, 1980), pp. 64—68.

[24]N. A. Ebrahim, C. Joshi, D. M. Villeneuve, N. H. Burnett, and M. C. Richardson, Phys. Rev. Lett. 43, 1995 (1979).

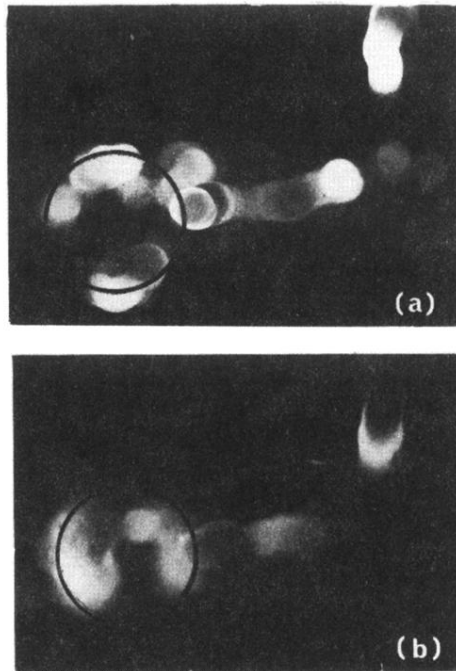[25]J. E. Crow, P. L. Auer, and J. E. Allen, J. Plasma Phys. 14, 65 (1975).

FIG. 7. Ion pinhole pictures of the rear surface of 2-mm-diam aluminum disks. Disks are mounted on L-shaped supports which extend to the right of the target and then up. Tracks due to fast ions are visible microscopically only on those bright areas on the target itself, not on the support structure. (a) Vertically polarized laser and (b) horizontally polarized laser.